TRIM35 ubiquitination regulates the expression of PKM2 tetramer and dimer and affects the malignant behaviour of breast cancer by regulating the Warburg effect

HAO WU[1,2], XINYI GUO[1], YILE JIAO[1], ZHENRU WU[2] and QING LV[1]

[1]Department of Breast Surgery, [2]Laboratory of Pathology, West China Hospital, Sichuan University, Chengdu, Sichuan 610041, P.R. China

Received June 29, 2022; Accepted September 13, 2022

DOI: 10.3892/ijo.2022.5434

Abstract. Breast cancer has become the leading cause of death in females. After comprehensive treatment, the lives of patients are still threatened by tumor metastasis and recurrence. Therefore, there is an urgent requirement to find an effective treatment target for breast cancer. Tripartite motif-containing 35 (TRIM35) is a ubiquitin ligase that has an important role in the recurrence and metastasis of malignant tumors. However, the role of TRIM35 in breast cancer has thus far remained elusive. The expression of TRIM35 was examined in a bioinformatics database and the effects of TRIM35 on the malignant biological behavior of breast cancer were analyzed by Cell Counting Kit-8, cell migration and invasion assays, flow cytometry and nude mouse xenograft experiments. It was determined that TRIM35 was downregulated in breast cancer tumor tissues and cell lines. Patients with low TRIM35 expression had shorter overall survival. Functional assays revealed that overexpression of TRIM35 inhibited the proliferation, migration and invasion, and promoted apoptosis of breast cancer cells. Furthermore, overexpression of TRIM35 was able to inhibit the Warburg effect in breast cancer cells. Mechanistic analyses indicated that TRIM35 regulates the transition of tetramers and dimers of pyruvate kinase M2 (PKM2) through ubiquitination and thereby affects the Warburg effect. In conclusion, the present results indicated that TRIM35 regulates the tetramer and dimer transition of PKM2 through ubiquitination and affects the malignant biological behavior of breast cancer by modulating the Warburg effect.

Correspondence to: Dr Qing Lv, Department of Breast Surgery, West China Hospital, Sichuan University, 37 Guoxue Lane, Chengdu, Sichuan 610041, P.R. China
E-mail: lvqing@wchscu.cn

Key words: TRIM35, breast cancer, tumorigenicity, PKM2, ubiquitination, Warburg effect

Introduction

As one of the most common malignant tumor types in females, breast cancer has exhibited a gradual increase in its incidence rate in recent years (1). In China, >300,000 females are diagnosed with breast cancer every year. In the eastern coastal areas and economically developed cities, the incidence rate of breast cancer has increased significantly (2). With the popularization of new treatment strategies and methods, the global mortality rate of breast cancer has gradually decreased (3). However, in China, particularly in the vast rural areas, the downward trend of breast cancer mortality is not significant. An important biological feature of breast cancer is its high metastatic capacity, which has become a major problem that limits the survival of patients with breast cancer and is associated with poor prognosis (4). It is of great significance to understand the specific mechanisms of breast cancer metastasis.

The tripartite motif-containing (TRIM) protein family is a member of the RING domain family of E3 ubiquitin ligases, which are composed of a RING-finger domain, two B-box domains and a C-terminal domain, and the presence of the RING domain suggests that TRIM proteins act as E3 ubiquitin linkages. Enzymes are involved in various physiological processes of cells (5,6). To date, >70 TRIM proteins have been found in humans and mice (7). They are encoded by ~71 genes and are divided into subfamilies I to XI according to their different domains (8). Previous studies have reported that TRIM proteins are extensively involved in a variety of cellular physiological processes (9-11). TRIM35, a member of the TRIM family, was found to have an important role in the malignant progression of tumors (12,13). In hepatocellular carcinoma (HCC), low TRIM35 expression promotes the malignant proliferation of HCC cells (14). Increasing the expression of TRIM35 may significantly inhibit cell proliferation, metastasis and invasion of breast cancer (15). However, the association between TRIM35 and the development of breast cancer has remained elusive. The aim of the present study was to examine the potential biological function of TRIM35 in the carcinogenesis of breast cancer.

Normally differentiated cells mainly rely on oxidative phosphorylation of mitochondria for cell energy supply, while most tumor cells rely on aerobic glycolysis (16). This

phenomenon is called the Warburg effect. The efficiency of aerobic glycolysis to produce ATP is low, but it gives tumor cells numerous advantages (17). Tumor cells grow rapidly, and excessive growth frequently puts tumor cells in a state of hypoxia, so they turn off the aerobic oxidation of mitochondria, and energy is provided by the anaerobic fermentation of glucose (18). Cells provide energy by enhancing anaerobic fermentation (19). After glucose is metabolized to pyruvate, it no longer undergoes aerobic oxidation through the tricarboxylic acid cycle of mitochondria, but is transformed into lactic acid through lactate dehydrogenase and discharged from cells (20). A study has indicated that Wilms tumor 1 associated protein enhances the stability of HK2 mRNA by binding to the 3'-UTR m6A site, which mediates the Warburg effect in gastric cancer to promote carcinogenesis (21). In triple-negative breast cancer, microRNA-210-3p regulates HIF-1α and p53 downstream glycolytic genes promote aerobic glycolysis and enhance the tumorigenicity of breast cancer cells (22). In colorectal tumors, condensin-2 complex subunit D3 increases the level of E2F transcription factor 1 (E2F1) and interacts with E2F1, recruiting more E2F1 to the promoter region of pyruvate dehydrogenase kinase 1 (PDK1) and PDK3 genes, resulting in the inhibition of pyruvate dehydrogenase activity and tricarboxylic acid cycle (23). It further promotes the reprogramming of glucose metabolism and enhances the Warburg effect in colorectal carcinogenesis and colorectal cancer progression (23). The above studies suggest that various mechanisms regulate the role of the Warburg effect in tumors. However, whether TRIM35 is related to the Warburg effect and the specific regulatory mechanism has remained elusive and was thus investigated in the present study.

Materials and methods

Patient samples. A total of 59 samples from patients with breast cancer (tumor tissues and paired normal adjacent tissues) were retrospectively obtained from the Department of Breast Surgery, West China Hospital, Sichuan University (Chengdu, China) between March 2019 and June 2020). The primary cancer tissues and the paired normal adjacent tissues were immediately snap-frozen in liquid nitrogen and stored at -80˚C until use for mRNA and protein analyses. The following exclusion criteria were used: i) Patients with incomplete pathological and clinical information; ii) patients with recurrent disease; iii) patients that had received preoperative radiation or chemotherapy, or any other treatment; iv) patients with other preoperative complications; v) patients with cognitive or mental disorders; and vi) pregnant women. The following inclusion criteria were used: i) Breast cancer tissue samples were all pathologically and confirmed as breast cancer. All patients provided written informed consent to participate in the study. The present study was approved by the Institutional Review Board of West China Hospital, Sichuan University (Chengdu, China).

Cell lines and cell culture. Human BC cell lines, including T47D, MDA-MB-231, MCF-7 and BT-474, and the human normal mammary epithelial cell line MCF-10A, were purchased from the American Type Culture Collection. T47D, MDA-MB-231, MCF-7 and BT-474 cells were cultured in DMEM (Gibco; Thermo Fisher Scientific, Inc.) containing 10% FBS (Biological Industries). MCF-10A cells were cultured in Minimum Essential Medium (cat. no. CC-3151; Lonza Group, Ltd.) supplemented with Mammary Epithelial Cell Growth Medium, MEGM® SingleQouts® (cat. no. CC-4136; Lonza Group, Ltd.) and 10% FBS (Biological Industries). Cells were cultured in a humidified atmosphere containing 5% CO_2 at 37˚C.

Cell transfection. Cells were transfected with the following plasmids: Overexpression TRIM35 (Oe-TRIM35), short hairpin (sh)RNA targeting TRIM35 for knockdown (Sh-TRIM35) and the respective negative controls (NCs) (Shanghai GenePharma, Co., Ltd.). Plasmids were transfected into breast cancer cells with Lipofectamine® 3000 (Invitrogen; Thermo Fisher Scientific, Inc.). The shRNA sequence De-TRIM35 was constructed into the pLVX-shRNA2-BSD lentiviral vector (Takara Bio USA, Inc.). The target sequences of the shRNAs were as follows: TRIM35 1, 5'-CTTGCATCT GTGGAATCTGTA-3'; TRIM35 2, 5'-AGTGTCAAGGAA GAACTGGAT-3'; TRIM35 3, 5'-GCGCTGGACCAGCTA CCG CTT-3' (this sequence was used to produce the main results); NC shRNA, 5'-TTCTCCGAACGTGTCACGTAA-3'. TRIM35-overexpressing lentiviruses (cat. no. CD527A-1; System Biosciences, LLC) were constructed into the lentiviral vector pCDH-EF1α-MCS-T2A-Puro (System Biosciences, LLC). For the NC group, empty vector was used as instead of the overexpression vector.

In another experiment, the cells were cultured in DMEM (10% FBS) containing the pyruvate kinase M2 (PKM2) activator TEPP-46 (5 μM) (cat. no. ML-265; Med Chem Express) for 24 h at 37˚C as directed by the manufacturer.

RNA extraction and reverse transcription-quantitative (RT-q) PCR. Total RNA was extracted from breast cancer tumor tissues, paired normal adjacent tissues and cell lines using TRIzol reagent (Takara Bio, Inc.). The extracted RNA was reverse transcribed to cDNA with PrimeScript RT Reagent (Takara Bio, Inc.) according to the manufacturer's instructions. Real-time qPCR was performed with a Prime-Script® RT Reagent Kit (Takara Bio, Inc.) according to the manufacturer's instructions and a LightCycler system (Roche Diagnostics) was used for detection with the following thermocycling conditions: Initial denaturation step at 95˚C for 3 min, followed by 45 cycles of denaturation at 95˚C for 20 sec, annealing at 60˚C for 30 sec and extension at 72˚C for 30 sec. GAPDH was used as an internal control. Relative RNA expression levels were calculated by the $2^{-\Delta\Delta Cq}$ method (24). The primer sequences were as follows: TRIM35 forward, 5'-CATCGCCAAGCA CAATCA GG-3' and reverse, 5'-GCGTTTTCGGCTCTT GTGTT-3'; GAPDH forward, 5'-GGAGCGACATCCGTC CAAAAT-3' and reverse, 5'-GGCTGTTGTCAATCTTCT CATGG-3'.

Western blot analysis. Total protein was isolated from breast cancer tumor tissues, paired normal adjacent tissues and cell lines using protein extraction buffer (RIPA lysis buffer; Beyotime Institute of Biotechnology). The nuclear protein was extracted using the nuclear protein extraction kit (cat. no. P0027; Beyotime Institute of Biotechnology)

according to the manufacturer's instructions. The protein concentration was quantified using a BCA kit (Beyotime Institute of Biotechnology) according to the manufacturer's protocol. Total protein was separated by 10% SDS-PAGE (20 μg protein per lane) and transfer onto a PVDF membrane (MilliporeSigma). The membranes were blocked for 1 h at room temperature with 5% nonfat milk powder (Beyotime Institute of Biotechnology). To detect the expression of PKM2 protein in different conformations, the total protein extracted from the sample could was not heat-denatured. Non-denatured gel sample loading buffer (Beyotime Institute of Biotechnology) was used for protein denaturation. In addition, protein electrophoresis was performed using native PAGE running buffer (Beyotime Institute of Biotechnology). The remaining experimental steps were the same as those of conventional western blot experiments. The membranes were probed at 4˚C overnight with antibodies against TRIM35 (cat. no. ab272582; 1:5,000 dilution; Abcam), PKM2 (cat. no. 15822-1-AP; ProteinTech Group, Inc.), Bax (cat. no. ab32503; 1:1,000 dilution; Abcam), Bcl-2 (cat. no. ab182858; 1:2,000 dilution; Abcam), N-cadherin (cat. no. ab76011; 1:5,000 dilution; Abcam), Ki-67 (cat. no. ab16667; 1:5,000 dilution; Abcam), E-cadherin (cat. no. ab40772; 1:10,000 dilution; Abcam), twist1 (cat. no. ab175430; 1:1,000 dilution; Abcam) and β-actin (cat. no. ab8226; 1:5,000 dilution; Abcam). The membranes were then incubated with the appropriate secondary antibodies (1:5,000 dilution; cat. nos. bs-40296G-HRP and bs-40295G-HRP; Bioss) for 1 h at room temperature. Finally, protein expression was analysed by chemiluminescence reagents (Hyperfilm ECL).

The Cancer Genome Atlas (TCGA) and the National Cancer Institute's Clinical Proteomic Tumor Analysis Consortium (CPTAC) analysis. The UALCAN database (http://ualcan.path.uab.edu/cgi-bin/ualcan-res.pl) was used to analyze the expression of TRIM35 in the TCGA and CPTAC datasets.

Protein-protein interaction network analysis. The Search Tool for the Retrieval of Interacting Genes and proteins (STRING; https://cn.string-db.org) was used to analyze the relationship between TRIM35 and PKM2.

Cell Counting Kit-8 (CCK-8) assay. Cells were transfected and then inoculated into 96-well plates ($2x10^3$ cells/well). After incubation for the indicated durations, CCK-8 assay reagent (Dojindo Molecular Technologies, Inc.) was added to each well containing cells and plates were incubated according to the manufacturer's instructions. The absorbance at 450 nm was recorded for each well using a microplate reader to determine cell proliferation.

Cell migration and invasion assays. Cell invasion and migration assays were performed using Transwell chambers (8 μm pore size; Costar; Corning, Inc.). MDA-MB-231 and MCF-7 cells ($1x10^5$ cells/well) were seeded into the upper chamber of the Transwell chambers with high-glucose DMEM containing 1% FBS. Furthermore, 500 μl of high-glucose DMEM containing 10% FBS was added to the matched lower chamber. After incubation for 48 h, various proportions of MDA-MB-231 and MCF-7 cells had moved to the lower chamber. The cells were fixed with methanol at room temperature for 30 min and stained with 0.1% crystal violet at room temperature for 20 min. For the invasion assay, the inserts were precoated with Matrigel® (1 mg/ml; Corning, Inc.).

Flow cytometric analysis of cell apoptosis. For cell apoptosis, after transfection, MDA-MB-231 and MCF-7 cells were seeded into 6-well plates. Once they reached confluence (60-70%), cells were collected and incubated with Annexin V-FITC (5 μl) (Biogot Technology Co., Ltd.) and propidium iodide (PI) solution (5 μl; Biogot Technology Co., Ltd.) at room temperature for 15 min according to the manufacturer's instructions. Cells were subsequently suspended in 400 μl binding buffer (Biogot Technology Co., Ltd.). Cell apoptosis progression was analyzed using flow cytometry (FACSAria; BD Biosciences). All data were analyzed with ModFit version 4.0 (Verity Software House, Inc.)

Glucose uptake assay. After transfection for 36 h, MDA-MB-231 and MCF-7 cells were incubated in DMEM without any L-glucose or phenol red for 8 h. The amount of glucose in the media was measured using a Glucose Colorimetric Assay kit (cat. no. K606-100; BioVision, Inc.) according to the manufacturer's instructions. Fresh DMEM (excluding L-glucose and phenol red) was used for the negative control. A total of three biological replicates were performed.

Intracellular pyruvate assay, lactate assay and ATP assay. After transfection for 36 h, MDA-MB-231 and MCF-7 cells were incubated in phenol red-free DMEM without FBS for 4 h. Subsequently, a pyruvate assay kit (cat. no. BC2205), lactate assay kit (cat. no. BC2235) and ATP assay kit (cat. no. BC0300; all from Beijing Solarbio Science & Technology Co., Ltd.) were used to measure intracellular concentrations of pyruvate, lactate and ATP, respectively, according to the manufacturer's instructions. The relative absorbance was measured using a spectrophotometer (Thermo Fisher Scientific, Inc.). The content of pyruvate, lactate and ATP were calculated according to the product manual.

Mouse xenograft tumor model. Female BALB/c-nu mice (total number, n=20; age, 5 weeks; weight, 20-25 g) were purchased from the Shanghai Experimental Animal Center and kept at the Experimental Animal Center of West China Hospital of Sichuan University (Chengdu, China). All animal experiments were performed in accordance with the institutional guidelines and were approved by the Committee on the Ethics of Animal Experiments of West China Hospital of Sichuan University (Chengdu, China). For the *in vivo* xenograft assay, MDA-MB-231 and MCF-7 cells ($5x10^6$) transfected with TRIM35 overexpression vector or control were subcutaneously injected into the mammary fat pads of the female athymic nude mice (n=5 in each group). Tumor growth was recorded once every four days with caliper measurements. Tumor volume was calculated according to the following formula: Volume=($width^2$ x length)/2. At 30 days after injection, the mice were euthanized and tumors were collected for analysis. For this, the mice were anesthetized with 1% pentobarbital sodium (45 mg/kg, intraperitoneal) and subsequently euthanized by cervical dislocation (when the heart had

stopped completely, the mouse was determined to be dead). Body weight loss >20% was considered a humane endpoint for euthanasia.

Co-immunoprecipitation (Co-IP). Cells were collected and lysed using RIPA Lysis Buffer (cat. no. P0013B; Beyotime Institute of Biotechnology) containing protease inhibitor (cat. no. P1011; Beyotime Institute of Biotechnology). Subsequently, 3 μg of antibody was added to the lysate and the mixture was incubated overnight at 4˚C. Protein A/G PLUS-Agarose beads (20 μl; cat. no. sc-2003; Santa Cruz Biotechnology, Inc.) were then added to the mixture and it was incubated on a rotator for 4 h at 4˚C. The bead-antibody-protein complexes were washed with precooled PBS three times and then boiled for subsequent western blot analysis (as described above). The antibodies used were as follows: PKM2 (cat. no. 15822-1-AP; 1:1,000 dilution; ProteinTech Group, Inc.) and TRIM35 (cat. no. ab272582; 1:1,000 dilution; Abcam).

Ubiquitination assay. MDA-MB-231 and MCF-7 cells were lysed in 1% SDS-containing RIPA buffer by sonication on ice. Lysates were then treated with Protein A/G Plus-Agarose (cat. no. sc-2003; Santa Cruz Biotechnology, Inc.) for 1 h at room temperature. Subsequently, each sample was incubated with IgG (cat. no. 30000-0-AP; 1:5,00 dilution; ProteinTech Group, Inc.) overnight at 4˚C. The nuclear pellet was collected by centrifugation at 10,000 x g for 5 min at 4˚C and subsequently washed four times using Protein A/G Plus-Agarose beads (by absorbing the protein, washing the beads and then releasing the protein again from the beads). The purified proteins were separated by gradient SDS-PAGE (as in the protocol for western blot analysis). Anti-PKM2 (cat. no. ab137852; 1:1,000 dilution; Abcam) or anti-ubiquitin antibody (cat. no. ab7780; 1:5,00 dilution; Abcam) was used for immunoblotting according to the protocol for western blot analysis.

Immunohistochemistry. Tissues were fixed in 10% formalin for 12 h at room temperature and embedded in paraffin for 8 h at room temperature. The slice thickness of the tissue specimen is 4um. The tissue specimen slides were deparaffinized twice with xylene for 15 min each at room temperature and rehydrated three times in a descending series of ethanol solutions (100, 100, 95 and 80%). Antigen retrieval was performed in 10 mmol/l sodium citrate solution (pH 6.0) at 100˚C for 16 min and the samples were then cooled for 30 min. Endogenous peroxidase activity was quenched using 3% hydrogen peroxide and blocking non-specific binding was performed with 5% goat serum (OriGene Technologies, Inc.) for 30 min at room temperature. Subsequently, the slides were incubated with anti-N-cadherin (cat. no. ab76011; 1:100 dilution; Abcam), anti-twist1 (cat. no. ab175430; 1:1,000 dilution; Abcam), anti-Ki-67 (cat. no. ab16667; 1:200 dilution; Abcam), anti-E-cadherin (cat. no. ab40772; 1:500 dilution; Abcam), anti-BCL-2 (cat. no. ab182858; 1:500 dilution; Abcam) and anti-BAX (cat. no. ab32503; 1:100 dilution; Abcam) at 4˚C overnight. Following the primary antibody incubation, slides were incubated with an anti-rabbit secondary IgG antibody (1:100; cat. no. SAP-9100; OriGene Technologies, Inc.) at 37˚C for 30 min. The samples were stained with 3,3-diaminobenzidine and Mayer's hematoxylin. Slides were visualized using a light microscope (magnification, x100 or x200; Zeiss AG). Immunostaining results were evaluated by two blinded pathologists. Staining was scored according to the percentage of positive cells and staining intensity. The scoring for staining intensity was as follows: 0, negative; 1, weak; 2, moderate; and 3, strong. The scoring system for the percentage of positive cells was as follows: Negative, 0-5%; 1, 6-25%; 2, 26-50%; 3, 51-75%; and 4, 76-100%. Sections with a total combined score of <4 were classified as having low expression, while sections with a score of ≥4 were considered to have high expression. From each tissue sample, 5 regions were randomly selected for evaluation.

Cell immunofluorescence. Cells were grown on coverslips that were coated with lysin. Cells (60% confluency) were fixed with 4% paraformaldehyde for 30 min at room temperature and permeabilized with 0.25% Triton X-100 solution for 20 min at room temperature. Cells were washed with PBS and then blocked in 5% bovine serum albumin (Beyotime Institute of Biotechnology) for 1 h at room temperature. Coverslips were incubated with antibodies against PKM2 (cat. no. 15822-1-AP; 1:1,000 dilution; ProteinTech Group, Inc.) overnight at 4˚C. After washing with PBS, cells were incubated with appropriate secondary antibody (cat. no. ab150077; 1:5,00 dilution; Abcam) for 1 h at room temperature and DAPI for 10 min at room temperature. Slides were imaged using an inverted fluorescence microscope.

Statistical analysis. All data were analyzed using SPSS 22.0 software (IBM Corporation) or GraphPad Prism version 7.0 (GraphPad Software, Inc.). Values are expressed as the mean ± standard deviation. Statistical differences (two groups) were analyzed by an unpaired Student's t-test. A paired Student's t-test was used to analyze the statistical difference of TRIM35 expression in breast cancer tissues and adjacent tissues. ANOVA was used for multiple-group comparisons and Tukey's test was used as the post-hoc test after ANOVA. $P<0.05$ was considered to indicate a statistically significant difference.

Results

TRIM35 is downregulated in breast cancer and low TRIM35 is associated with unfavorable survival in patients. Analysis of the TCGA and GEPIA datasets indicated that TRIM35 was low in breast cancer (Fig. 1A and B). In tissue samples collected from patients with breast cancer (age range, 27-76 years; all patients were female; demographic and clinicopathological data provided in Table SI), western blot and RT-qPCR analyses suggested that the expression of TRIM35 in breast cancer tissues was lower than that in adjacent tissues (Fig. 1C and D). Furthermore, the expression level of TRIM35 in breast cancer cell lines was significantly lower than that in the normal breast cell line (Fig. 1E). Through the analysis of the relationship between the expression of TRIM35 and the prognosis of patients with breast cancer in the GEO and TCGA databases, it was revealed that those patients with low TRIM35 expression exhibited significantly shorter overall survival than those with high TRIM35 expression (Fig. 1F and G).

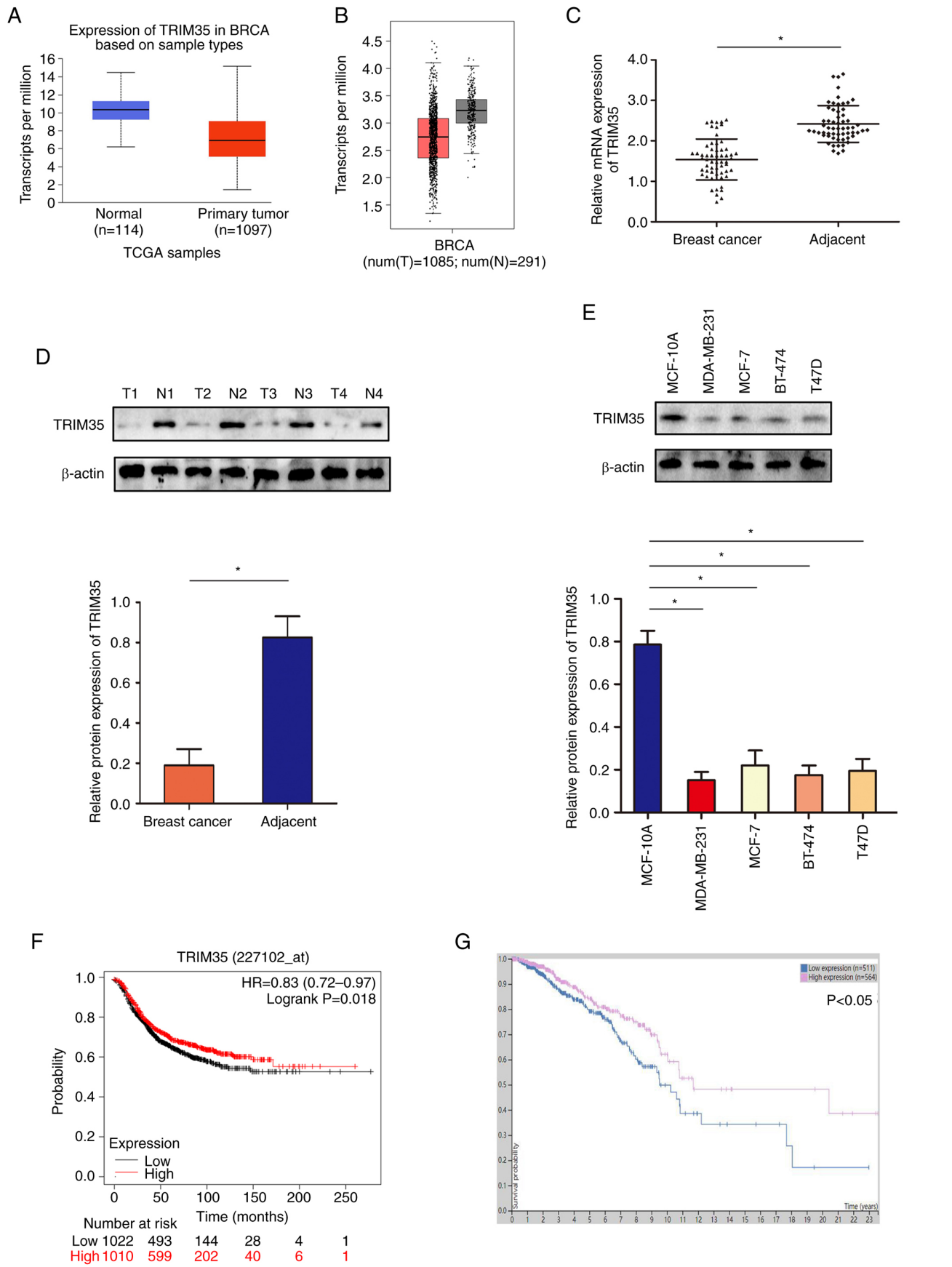

Figure 1. Expression profile of TRIM35 in breast cancer and its clinical relevance. (A) mRNA expression of TRIM35 in TCGA database. (B) mRNA expression of TRIM35 in the GEPIA database. (C) mRNA expression of TRIM35 in breast cancer samples. (D) The protein expression of TRIM35 in breast cancer samples. (E) TRIM35 protein expression in breast cancer cell lines. (F) Kaplan-Meier curves indicating the relationship between TRIM35 expression and the prognosis of patients with breast cancer in TCGA database. (G) Kaplan-Meier curves indicating the relationship between the expression of TRIM35 and the prognosis of patients with breast cancer in the GEPIA database. *P<0.05. TRIM35, tripartite motif-containing 35; TCGA, The Cancer Genome Atlas; T, tumor sample; N, normal tissue sample; HR, hazard ratio; BRCA, breast cancer.

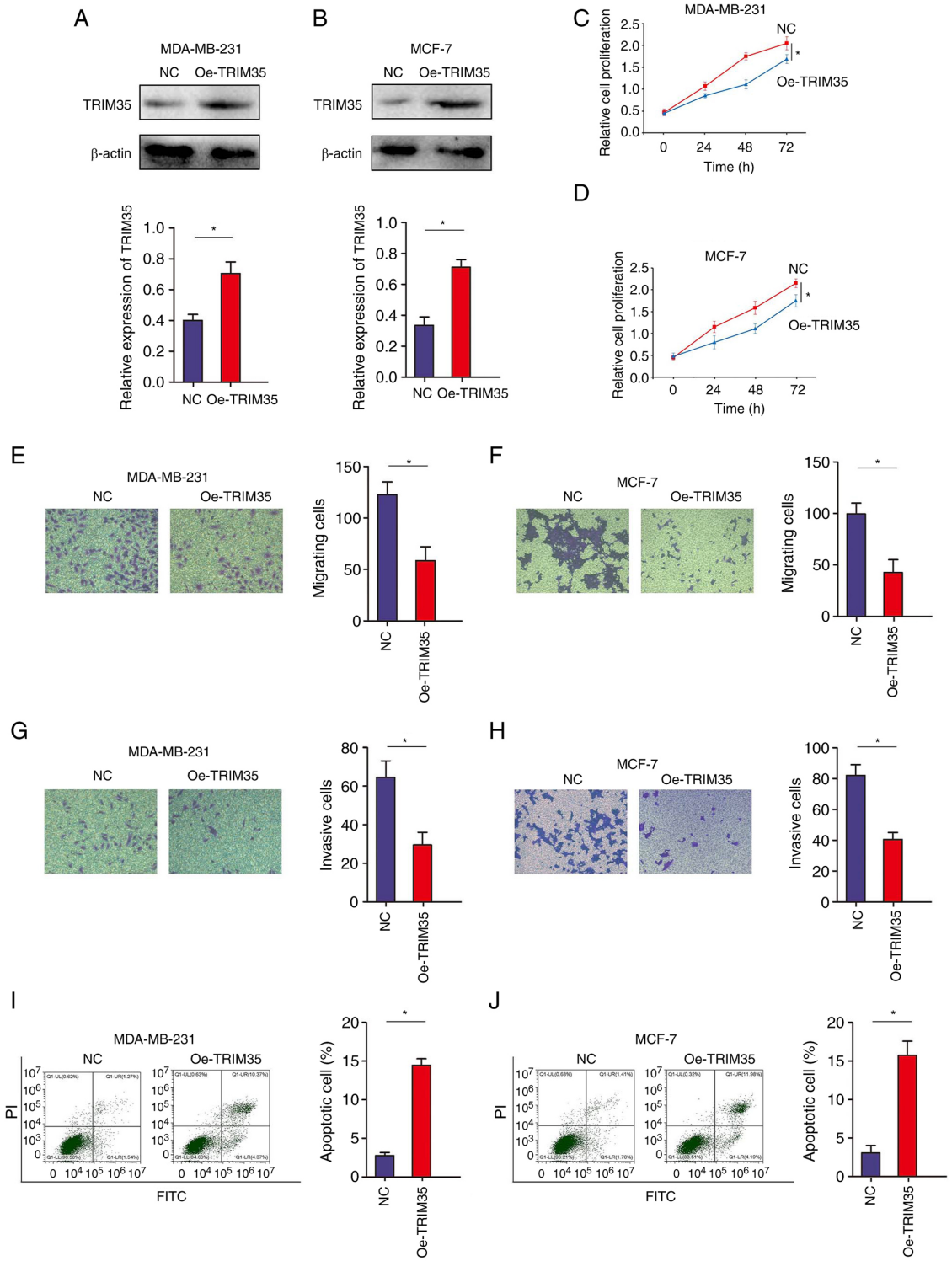

Figure 2. TRIM35 significantly suppresses cell proliferation, migration and invasion and promotes apoptosis in breast cancer cell lines. (A) Western blot assay indicating the protein expression of TRIM35 in MD-MBA-231 cells. (B) Western blot assay quantifying the protein expression of TRIM35 in MCF-7 cells. (C) CCK-8 assay to detect the proliferation of MD-MBA-231 cells. (D) CCK-8 assay to detect the proliferation of MCF-7 cells. Transwell assays to detect (E) MD-MBA-231 cell migration, (F) MCF-7 cell migration, (G) MD-MBA-231 cell invasion and (H) MCF-7 cell invasion (magnification, x200). (I) Flow cytometry was used to examine the effects of TRIM35 overexpression on MD-MBA-231 cell apoptosis. (J) Flow cytometry was used to examine the effects of TRIM35 overexpression on MCF-7 cell apoptosis. *P<0.05. TRIM35, tripartite motif-containing 35; NC, negative control; Oe, overexpression; CCK-8, Cell Counting Kit-8; PI, propidium iodide.

TRIM35 overexpression inhibits breast cancer cell proliferation, migration and invasion and promotes apoptosis. To further verify the role of TRIM35 in breast cancer malignancy, gain-of-function experiments were performed in MDA-MB-231 and MCF-7 cell lines. It was confirmed that TRIM35 was effectively overexpressed in MDA-MB-231 and MCF-7 cell lines (Fig. 2A and B). The CCK-8 assay indicated that increasing the expression of TRIM35 inhibited number

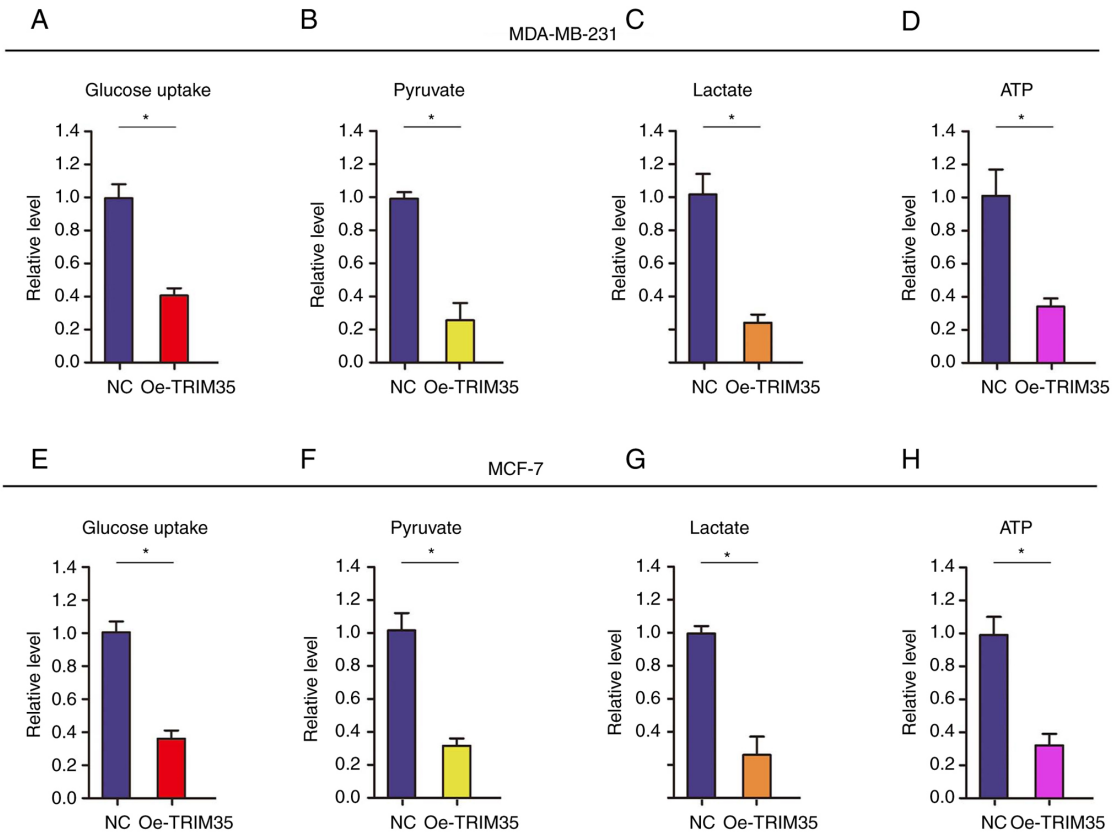

Figure 3. TRIM35 impedes the energy metabolism in breast cancer cells. Examination of the effects of TRIM35 overexpression on (A) glucose uptake, (B) pyruvate, (C) lactate and (D) ATP in MD-MBA-231 cells. Examination of the effects of TRIM35 overexpression on (E) glucose uptake, (F) pyruvate, (G) lactate and (H) ATP in MCF-7 cells. *P<0.05. TRIM35, tripartite motif-containing 35; NC, negative control; Oe, overexpression.

of viable MDA-MB-231 and MCF-7 cells (Fig. 2C and D). The efficacy of TRIM35 overexpression and silencing using multiple clones are provided in Figs. S1 and S2. Furthermore, a Transwell assay suggested that increasing the expression of TRIM35 significantly inhibited the migration of MDA-MB-231 and MCF-7 cells (Fig. 2E and F). In addition, Transwell experiments indicated that increasing the expression of TRIM35 significantly inhibited the invasion of MDA-MB-231 and MCF-7 cells (Fig. 2G and H). Increasing the expression of TRIM35 promoted the apoptosis of MDA-MB-231 and MCF-7 cells (Fig. 2I and J). However, knockdown of TRIM35 promoted the malignant biological behavior of breast cancer cells (Fig. S3).

TRIM35 overexpression impedes energy metabolism by restraining glycolysis in breast cancer cells. Metabolic reprogramming of tumor cells is an important biological change, mainly manifested as enhanced glycolysis, which provides effective energy and metabolites for the rapid growth of tumor cells in different microenvironments (25,26).

In the present study, it was analyzed whether TRIM35 affects glycolysis in breast cancer cells. The level of glucose uptake was tested (Fig. 3), revealing that it was significantly decreased after TRIM35-overexpression in MDA-MB-231 and MCF-7 cells (Fig. 3A and E). In addition, the levels of related metabolites, i.e. pyruvate and lactate, as well as the production of ATP, were tested. The results revealed that the levels of pyruvate and lactate, and the production of ATP were all significantly decreased in TRIM35-overexpressing MDA-MB-231 (Fig. 3B-D) and MCF-7 cells (Fig. 3F-H).

TRIM35 overexpression inhibits breast cancer cell proliferation in vivo. The *in vivo* experiments indicated that overexpression of TRIM35 significantly inhibited the growth of tumors derived from MDA-MB-231 breast cancer cells (Fig. 4A-C). In addition, western blot indicated that overexpression of TRIM35 significantly inhibited the expression of N-cadherin, Twist1, Bcl-2 and Ki-67, while significantly promoting the expression of E-cadherin and Bax in MDA-MB-231-cell tumors (Fig. 4D). In line with the above results, in tumors derived from MCF-7 cells with overexpression of TRIM35, tumor growth was significantly inhibited (Fig. 4E-G) and the expression of N-cadherin, Twist1, Bcl-2 and Ki-67 were significantly inhibited, while the expression levels of E-cadherin and Bax were significantly promoted (Fig. 4H). Immunohistochemical staining also confirmed the above results (Fig. S4).

TRIM35 combines with PKM2 and participates in the regulation of PKM2 in breast cancer. As a key protein of the Warburg effect, PKM2 is widely involved in the glycolysis process of tumor cells (27,28). The above-mentioned results of the present study indicated that TRIM35 significantly regulates the glycolysis process in breast cancer. Therefore, it was further examined whether TRIM35 has a regulatory effect on PKM2.

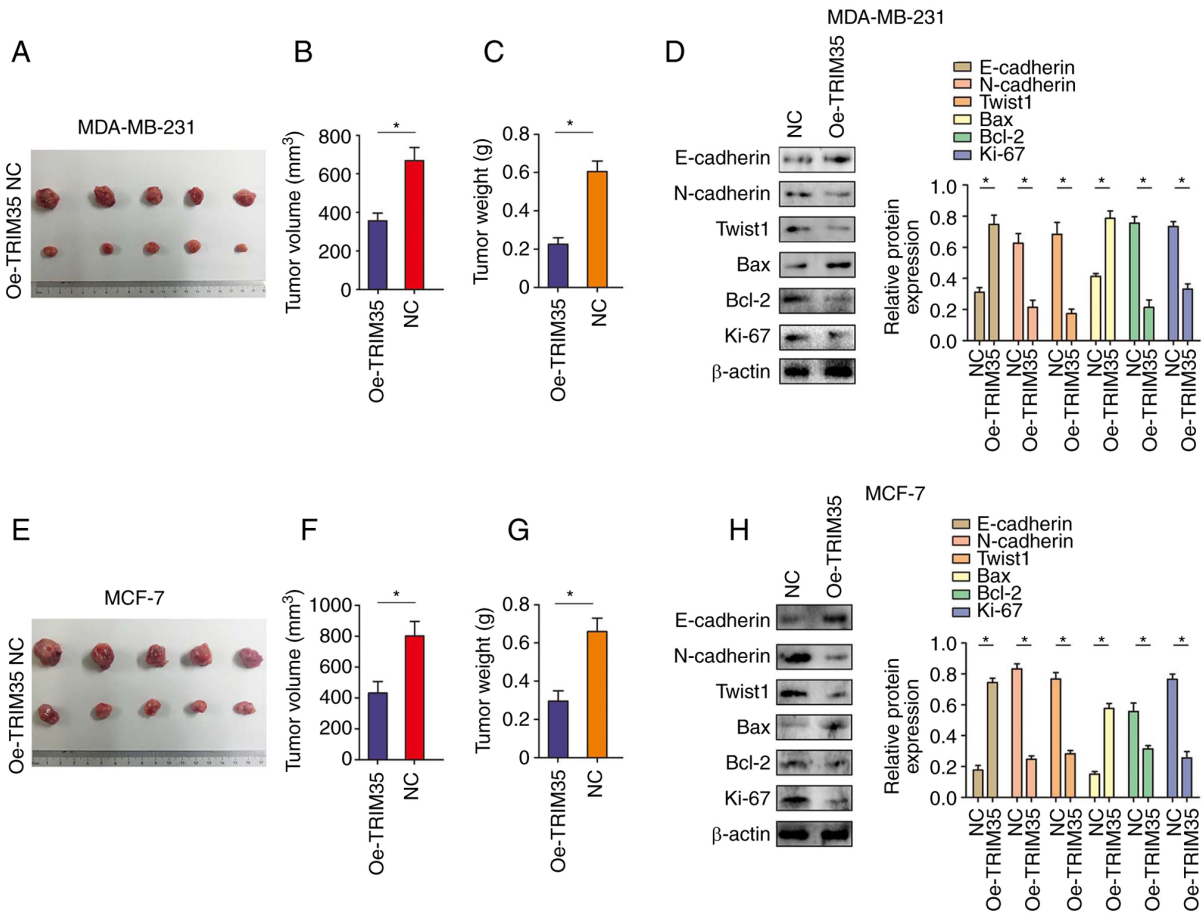

Figure 4. TRIM35 overexpression inhibits breast cancer cell proliferation *in vivo*. (A) Representative images of excised xenograft tumors grown on nude mice from MDA-MB-231 cells, which had increased expression of TRIM35. (B) Xenograft tumor volume in each group derived from MDA-MB-231 cells with increased expression of TRIM35. (C) Tumor weight in each group derived from MDA-MB-231 cells with increased expression of TRIM35. (D) Western blot analysis revealed the expression of EMT components, including proliferation- and apoptosis-related indicators in MDA-MB-231 cells with increased expression of TRIM35. (E) Representative images of excised xenograft tumors grown on nude mice from MCF-7 cells with increased expression of TRIM35. (F) Tumor volume in each group derived from MCF-7 cells with increased expression of TRIM35. (G) Tumor weight in each group derived from MCF-7 cells with increased expression of TRIM35. (H) Western blot analysis revealed the expression of EMT components, including proliferation- and apoptosis-related indicators in MCF-7 cells with increased the expression of TRIM35. *P<0.05. TRIM35, tripartite motif-containing 35; NC, negative control; Oe, overexpression; EMT, epithelial-to-mesenchymal transition.

The relationships between TRIM35 and PKM2 were verified by using reciprocal Co-IP experiments carried out in MDA-MB-231 and MCF-7 cells. The results confirmed the interaction between endogenous TRIM35 and PKM2 (Fig. 5A and B). Subsequently, a protein-protein interaction network prediction was performed, suggesting that TRIM35 had a significant binding regulatory effect on PKM2 (Fig. S5). However, no changes in the mRNA or protein levels of PKM2 were observed after changing the expression of TRIM35 (Fig. 5C-F).

TRIM35 regulates the ubiquitination of PKM2, altering its tetramer-dimer ratio and promoting the Warburg effect. PKM2 functions to convert phosphoenolpyruvate (PEP) to pyruvate in the final step of glycolysis (29). Three dynamic types of PKM2 exist in mammalian cells, namely monomeric, dimeric and tetrameric PKM2s, but only dimeric and tetrameric PKM2s have pyruvate kinase activity (30). Monomeric PKM2 is in an inactive state. Dimeric PKM2 drives glucose-derived carbon towards glycolysis (30). Tetrameric PKM2 promotes the transfer of glucose-derived carbons in the direction of the respiratory chain (31). The above-mentioned results of the present study indicated that glycolytic function was inhibited after overexpression of TRIM35, which also suggested that the changes in tetramers and dimers of PKM2 may be the key target of TRIM35 in regulating PKM2.

Since TRIM35 is an ubiquitin E3 ligase, it was further hypothesized that TRIM35 regulates the expression of PKM2 at the translational or post-translational level (32). Specifically, in the present study, it was investigated whether TRIM35 affects the tetramer and dimer changes of PKM2 by mediating changes in ubiquitination.

First, dimers of PKM2 were indicated to be highly expressed in breast cancer cell lines (Fig. S6A-D). The ubiquitination levels of PKM2 were enhanced in both the MDA-MB-231 and MCF-7 cell lines with TRIM35 overexpression, which suggests that TRIM35 overexpression allowed more PKM2 to enter the degradation process (Fig. 6A and B). In addition, the change in ubiquitination has a regulatory role in the change in tetramers and dimers of PKM2. Therefore, the effect of the change of ubiquitination on the expression of PKM2 tetramer and dimer was further analyzed. Overexpression of TRIM35

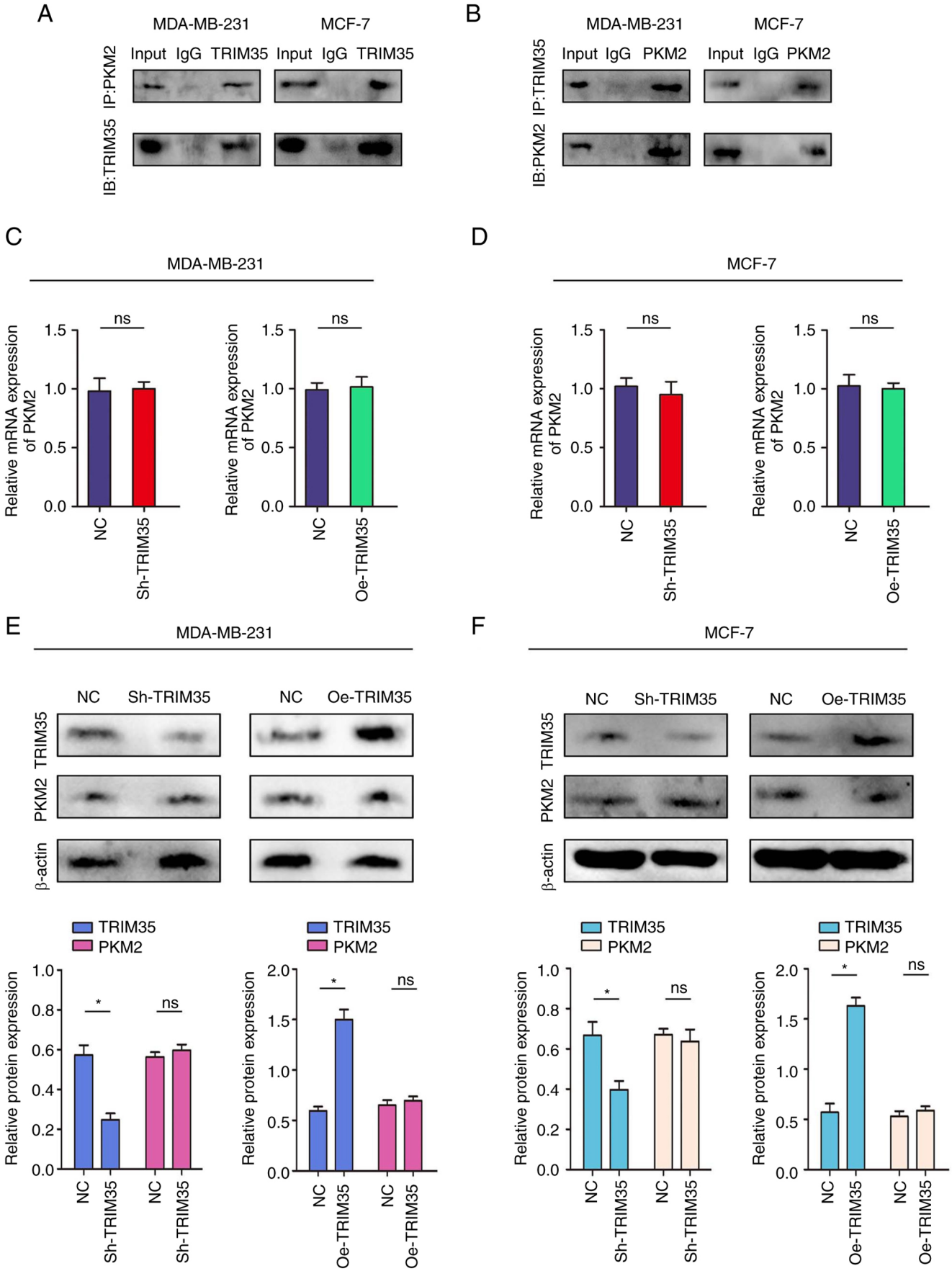

Figure 5. TRIM35 combines with PKM2. (A) Co-IP experiments indicated that TRIM35 interacted with PKM2 in the MDA-MB-231 and MCF-7 cell lines. (B) The Co-IP experiments indicated that TRIM35 interacted with PKM2 in the MDA-MB-231 and MCF-7 cell lines. (C-F) TRIM35 was overexpressed or knocked down. (C) mRNA expression of PKM2 in MDA-MB-231 cells. (D) mRNA expression of PKM2 in MCF-7 cells. (E) Protein expression of TRIM35 and PKM2 in MDA-MB-231 cells. (F) Protein expression of TRIM35 and PKM2 in MCF-7 cells. *P<0.05; ns, no significance; TRIM35, tripartite motif-containing 35; IB, immunoblot; IP, immunoprecipitation; NC, negative control; Oe, overexpression; sh, short hairpin RNA; PKM2, pyruvate kinase M2.

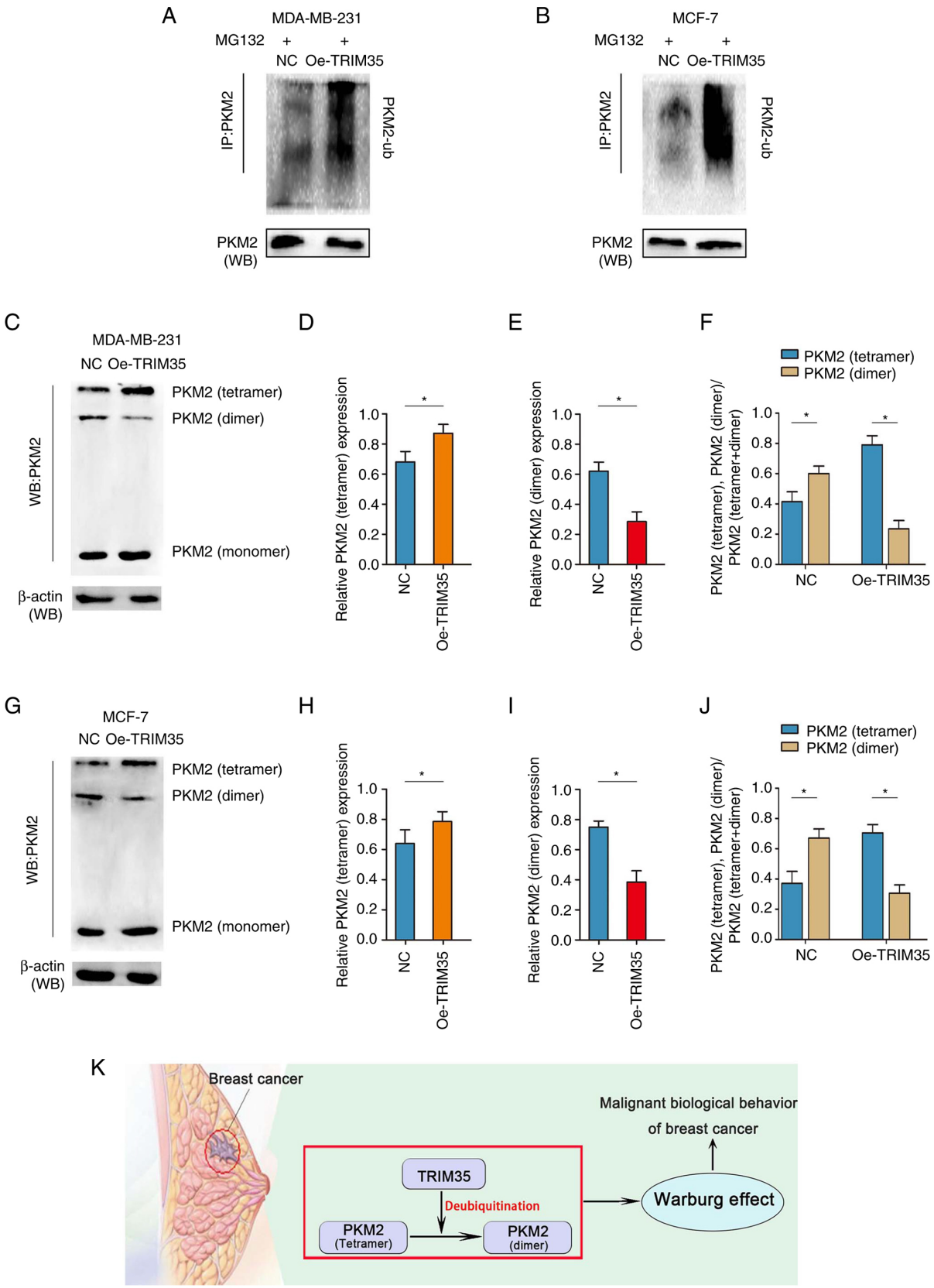

Figure 6. TRIM35 regulates the tetramer-dimer transition of PKM2 through ubiquitination, thereby regulating the Warburg effect. (A) The levels of PKM2-ub were examined by western blot with anti-ubiquitin antibody in MDA-MB-231 cells. (B) The levels of PKM2-ub were examined by western blot with anti-ubiquitin antibody in MCF-7 cells. (C) Western blot analysis of the protein expression levels of monomeric, dimeric and tetrameric PKM2 in MDA-MB-231 cells. (D) Relative expression of tetrameric PKM2 in MDA-MB-231 cells. (E) Relative expression of dimeric PKM2 in MDA-MB-231 cells. (F) Proportion of PKM2 tetramers and PKM2 dimers in MDA-MB-231 cells. (G) Western blot analysis of the protein expression levels of monomeric, dimeric and tetrameric PKM2 in MCF-7 cells. (H) Relative expression of tetrameric PKM2 in MCF-7 cells. (I) Relative expression of dimeric PKM2 in MCF-7 cells. (J) Proportion of PKM2 tetramers and PKM2 dimers in MCF-7 cells. (K) Schematic illustration of TRIM35 regulating the tetramer-dimer transition of PKM2 through ubiquitination, thereby regulating the Warburg effect. *P<0.05. TRIM35, tripartite motif-containing 35; IP, immunoprecipitation; NC, negative control; Oe, overexpression; PKM2, pyruvate kinase M2; PKM2-ub, ubiquitinated PKM2 protein; WB, western blot.

significantly increased the expression of PKM2 tetramer, decreased the expression of PKM2 dimer and increased the ratio of PKM2 tetramer in MDA-MB-231 cells (Fig. 6C-F). The same results were also obtained in MCF-7 cells (Fig. 6G-J). Furthermore, knockdown of TRIM35 significantly decreased the expression of PKM2 tetramer, increased the expression of PKM2 dimer and decreased the ratio of PKM2 tetramer in MDA-MB-231 and MCF-7 cells (Fig. S7A-H). When PKM2 dimer was reduced, PKM2 translocated from the nucleus to the cytoplasm (Fig. S8A-D). The PKM2 activator TEPP-46 has been reported to reduce dimer formation and promote tetramer formation (33). Of note, treatment of breast cancer cells with TEPP-46 significantly inhibited number of viable cells (33), migration and invasion and promoted cell apoptosis (Fig. S9). Collectively, these data suggest that TRIM35 affects the expression of the PKM2 tetramer and dimer by regulating the ubiquitination of PKM2 and regulates the Warburg effect to promote the malignant biological behavior of breast cancer (Fig. 6K).

Discussion

Ubiquitination modification is one of the important modifications of eukaryotic regulatory proteins after translation (34). It affects cell proliferation, differentiation, signal transduction and other important physiological activities through the degradation, localization and functional regulation of proteins (35). A series of processes of protein ubiquitination modification are mainly completed by the ubiquitin proteasome complex composed of ubiquitin activating enzyme E1, ubiquitin binding enzyme E2 and ubiquitin ligase E3 (34). Most of the modified target proteins are then degraded by the 26S proteasome (35). This process is called the ubiquitin proteasome pathway. However, in recent years, an increasing number of studies have indicated that ubiquitin modification is widely involved in the assembly of signal pathway protein complexes and the protein transport, as well as the activation and inactivation of enzymes, which has made research on ubiquitin modification in tumor signal transduction mechanisms a hot spot in this field (36,37). Among the proteins that perform ubiquitin modification, E3 ubiquitin ligase has become a potential anti-tumor target due to its specific recognition of target proteins. As a key protein of E3 ubiquitin ligase, TRIM35 is widely involved in the regulation of various physiological and pathological processes in tumors (38). In non-small cell lung cancer, the expression of TRIM35 was observed to be increased in tumor samples, and high expression of TRIM35 was closely related to poor clinical prognosis of patients (39). Inhibition of TRIM35 expression in non-small cell lung cancer cell lines promoted cell proliferation, migration and invasion (39). Another study reported that E3 ubiquitin ligase TRIM35 is expressed at a low level in diffuse large B-cell lymphoma (40). Overexpression of TRIM35 inhibited the proliferation of diffuse large B-cell lymphoma cells. A mechanistic study demonstrated that TRIM35 mediates ubiquitination and degradation of 'clock', a key regulator of the circadian rhythm (40). The present study further indicated that the expression of TRIM35 was lower in breast cancer and its low expression was associated with poor prognosis. A functional study performed as part of the present paper indicated that overexpression of TRIM35 significantly inhibited proliferation, migration and invasion and promoted apoptosis of breast cancer cells.

The Warburg effect is the main mode of ATP production in tumor cells (41). It changes from mitochondrial oxidative phosphorylation of glucose to aerobic glycolysis (41). Its essence is the rearrangement of the energy metabolism in tumor cells (41). Pyruvate kinase is the ultimate rate-limiting enzyme in glycolysis (42). PKM2 is the key enzyme in the Warburg effect (42). It is able catalyze PEP to transfer phosphate groups to adenosine diphosphate to generate ATP (43). PKM2 has two conformations in cells, a high enzyme activity tetramer and a low enzyme activity dimer (44). The low enzyme activity of the dimer is a necessary condition to ensure the Warburg effect (44). The low enzyme activity of PKM2 helps to make carbon atoms bind to bioactive substances more rapidly, promote the rapid energy production of glycolytic intermediates and enter the collateral pathway, synthesize nucleic acids, amino acids and lipids without accumulating reactive oxygen species, and provide energy and metabolites for the malignant growth of tumor cells (44). Protein conformation and function are closely related to posttranscriptional modification, which frequently includes ubiquitination, phosphorylation and acetylation (45). Zheng *et al* (46) indicated that special at rich sequence binding protein 1 was ubiquitinated through its N-terminal ubiquitin-like domain, maintaining the tetramer structure and having the role of an oncogene. French *et al* (47) observed that ubiquitination modification may promote the formation of casein kinase II tetramer and inhibit the proliferation of tumor cells. The present results are consistent with those of previous studies (43,44) with regard to the expression of PKM2 dimer being inhibited, the expression of PKM2 tetramer being promoted, and the proliferation, invasion and migration of breast cancer cells being inhibited after treatment of breast cancer cells with TEPP-46, while apoptosis was increased. It was suggested that the conversion of PKM2 tetramer and dimer has an important role in the malignant biological behavior of breast cancer. But more importantly, the present results suggested that TRIM35 is able to regulate the ubiquitination modification of PKM2 and promote its transformation from dimers to tetramers, inhibiting the Warburg effect and reducing glycolysis in tumor cells. Of course, there are still limitations to the present study. There are numerous key enzymes in the glycolysis pathway involved in the Warburg effect, but in the present study, only the regulatory mechanism of TRIM35 on PKM2 was analyzed, while it was not analyzed whether TRIM35 has a regulatory effect on other key enzymes. Future research by our group will focus on the impact of TRIM35 on other key enzymes of the Warburg effect.

Taken together, the results of the present study indicated that the TRIM35-PKM2 axis promotes an aggressive phenotype in tumors by enhancing glycolysis. TRIM35 is a potential target for coordinating glycolysis in breast cancer. Protein ubiquitination may be a key mechanism by which TRIM35 regulates the transition between tetramers and dimers of PKM2.

Acknowledgements

Not applicable.

Funding

The present study was supported by the National Natural Science Foundation of China (grant no. 82100655), Key Research and Development Projects of the Sichuan Science and Technology Department (grant no. 22QYCX0129) and Key Research and Development Projects of the Sichuan Science and Technology Department (grant no. 22ZDYF1209).

Availability of data and materials

The datasets used and/or analyzed during the current study are available from the corresponding author on reasonable request.

Authors' contributions

HW and QL conceived and designed the study. XG, YJ and ZW performed the experiments. HW and QL analyzed the data. HW and QL wrote the manuscript. HW and QL checked and approved the authenticity of the raw data. All authors read and approved the final manuscript.

Ethics approval and consent to participate

The study was conducted with the approval of the Ethics Committee of West China Hospital, Sichuan University (Chengdu, China). Written informed consent was obtained from all patients for the use of their tissue in this study.

Patient consent for publication

Not applicable.

Competing interests

The authors declare that they have no competing interests.

References

1. Harbeck N and Gnant M: Breast cancer. Lancet 389: 1134-1150, 2017.
2. Fan L, Strasser-Weippl K, Li JJ, St Louis J, Finkelstein DM, Yu KD, Chen WQ, Shao ZM and Goss PE: Breast cancer in China. Lancet Oncol 15: e279-e289, 2014.
3. Barzaman K, Karami J, Zarei Z, Hosseinzadeh A, Kazemi MH, Moradi-Kalbolandi S, Safari E and Farahmand L: Breast cancer: Biology, biomarkers, and treatments. Int Immunopharmacol 84: 106535, 2020.
4. Veronesi U, Boyle P, Goldhirsch A, Orecchia R and Viale G: Breas cancer. Lancet 365: 1727-1741, 2005.
5. Hatakeyama S: TRIM family proteins: Roles in autophagy, immunity, and carcinogenesis. Trends Biochem Sci 42: 297-311, 2017.
6. Zhao G, Liu C, Wen X, Luan G, Xie L and Guo X: The translational values of TRIM family in pan-cancers: From functions and mechanisms to clinics. Pharmacol Ther 227: 107881, 2021.
7. Zhan W and Zhang S: TRIM proteins in lung cancer: Mechanisms, biomarkers and therapeutic targets. Life Sci 268: 118985, 2021.
8. Meroni G: TRIM E3 ubiquitin ligases in rare genetic disorders. Adv Exp Med Biol 1233: 311-325, 2020.
9. Venuto S and Merla G: E3 ubiquitin ligase TRIM proteins, cell cycle and mitosis. Cells 8: 510, 2019.
10. Goyani S, Roy M and Singh R: TRIM-NHL as RNA binding ubiquitin E3 ligase (RBUL): Implication in development and disease pathogenesis. Biochim Biophys Acta Mol Basis Dis: Jan 6, 2021 (Epub ahead of print).
11. Connacher RP and Goldstrohm AC: Molecular and biological functions of TRIM-NHL RNA-binding proteins. Wiley Interdiscip Rev RNA 12: e1620, 2021.
12. Eberhardt W, Haeussler K, Nasrullah U and Pfeilschifter J: Multifaceted roles of TRIM proteins in colorectal carcinoma. Int J Mol Sci 21: 7532, 2020.
13. Watanabe M and Hatakeyama S: TRIM proteins and diseases. J Biochem 161: 135-144, 2017.
14. Chen Z, Wang Z, Guo W, Zhang Z, Zhao F, Zhao Y, Jia D, Ding J, Wang H, Yao M and He X: TRIM35 Interacts with pyruvate kinase isoform M2 to suppress the warburg effect and tumorigenicity in hepatocellular carcinoma. Oncogene 34: 3946-3956, 2015.
15. Wang R, Huang KL and Xing LX: TRIM35 functions as a novel tumor suppressor in breast cancer by inducing cell apoptosis through ubiquitination of PDK1. Neoplasma 69: 370-382, 2022.
16. Shulman RG and Rothman DL: The glycogen shunt maintains glycolytic homeostasis and the warburg effect in cancer. Trends Cancer 3: 761-767, 2017.
17. Lebelo MT, Joubert AM and Visagie MH: Warburg effect and its role in tumourigenesis. Arch Pharm Res 42: 833-847, 2019.
18. Kozal K, Jóźwiak P and Krześlak A: Contemporary perspectives on the warburg effect inhibition in cancer therapy. Cancer Control: Sep 23, 2021 (Epub ahead of print).
19. Johar D, Elmehrath AO, Khalil RM, Elberry MH, Zaky S, Shalabi SA and Bernstein LH: Protein networks linking warburg and reverse warburg effects to cancer cell metabolism. Biofactors 47: 713-728, 2021.
20. Zam W, Ahmed I and Yousef H: The warburg effect on cancer cells survival: The role of sugar starvation in cancer therapy. Curr Rev Clin Exp Pharmacol 16: 30-38, 2021.
21. Yu H, Zhao K, Zeng H, Li Z, Chen K, Zhang Z, Li E and Wu Z: N6-methyladenosine (m6A) methyltransferase WTAP accelerates the warburg effect of gastric cancer through regulating HK2 stability. Biomed Pharmacother 133: 111075, 2021.
22. Du Y, Wei N, Ma R, Jiang S and Song D: A miR-210-3p regulon that controls the warburg effect by modulating HIF-1α and p53 activity in triple-negative breast cancer. Cell Death Dis 11: 731, 2020.
23. Jing Z, Liu Q, He X, Jia Z, Xu Z, Yang B and Liu P: NCAPD3 enhances warburg effect through c-myc and E2F1 and promotes the occurrence and progression of colorectal cancer. J Exp Clin Cancer Res 41: 198, 2022.
24. Livak KJ and Schmittgen TD: Analysis of relative gene expression data using real-time quantitative PCR and the 2(-Delta Delta C(T)) method. Methods 25: 402-408, 2001.
25. Ganapathy-Kanniappan S and Geschwind JF: Tumor glycolysis as a target for cancer therapy: Progress and prospects. Mol Cancer 12: 152, 2013.
26. Vander Heiden MG, Cantley LC and Thompson CB: Understanding the warburg effect: The metabolic requirements of cell proliferation. Science 324: 1029-1033, 2009.
27. Dayton TL, Jacks T and Vander Heiden MG: PKM2, cancer metabolism, and the road ahead. EMBO Rep 17: 1721-1730, 2016.
28. Zhu S, Guo Y, Zhang X, Liu H, Yin M, Chen X and Peng C: Pyruvate kinase M2 (PKM2) in cancer and cancer therapeutics. Cancer Lett 503: 240-248, 2021.
29. Zhang Z, Deng X, Liu Y, Liu Y, Sun L and Chen F: PKM2, function and expression and regulation. Cell Biosci 9: 52, 2019.
30. Zahra K, Dey T, Ashish, Mishra SP and Pandey U: Pyruvate kinase M2 and cancer: The role of PKM2 in promoting tumorigenesis. Front Oncol 10: 159, 2020.
31. He X, Du S, Lei T, Li X, Liu Y, Wang H, Tong R and Wang Y: PKM2 in carcinogenesis and oncotherapy. Oncotarget 8: 110656-110670, 2017.
32. Ikeda K and Inoue S: TRIM proteins as RING finger E3 ubiquitin ligases. Adv Exp Med Biol 770: 27-37, 2012.
33. Anastasiou D, Yu Y, Israelsen WJ, Jiang JK, Boxer MB, Hong BS, Tempel W, Dimov S, Shen M, Jha A, *et al*: Pyruvate kinase M2 activators promote tetramer formation and suppress tumorigenesis. Nat Chem Biol 8: 839-847, 2012.
34. Popovic D, Vucic D and Dikic I: Ubiquitination in disease pathogenesis and treatment. Nat Med 20: 1242-1253, 2014.
35. Cockram PE, Kist M and Prakash S: Ubiquitination in the regulation of inflammatory cell death and cancer. Cell Death Differ 28: 591-605, 2021.
36. Zou T and Lin Z: The involvement of ubiquitination machinery in cell cycle regulation and cancer progression. Int J Mol Sci 22: 5754, 2021.

37. Senft D, Qi J and Ronai ZA: Ubiquitin ligases in oncogenic transformation and cancer therapy. Nat Rev Cancer 18: 69-88, 2018.
38. Jia D, Wei L, Guo W, Zha R, Bao M, Chen Z, Zhao Y, Ge C, Zhao F, Chen T, *et al*: Genome-wide copy number analyses identified novel cancer genes in hepatocellular carcinoma. Hepatology 54: 1227-1236, 2011.
39. Zhang J, Xu Z, Yu B, Xu J and Yu B: Tripartite motif containing 35 contributes to the proliferation, migration, and invasion of lung cancer cells in vitro and in vivo. Biosci Rep: Apr 30, 2020 (Epub ahead of print).
40. Tan X, Cao F, Tang F, Lu C, Yu Q, Feng S, Yang Z, Chen S, He X, He J, *et al*: Suppression of DLBCL Progression by the E3 ligase Trim35 is mediated by CLOCK degradation and NK cell infiltration. J Immunol Res 24: 9995869, 2021.
41. Liberti MV and Locasale JW: The warburg effect: How does it benefit cancer cells? Trends Biochem Sci 41: 211-218, 2016.
42. Lu Z and Hunter T: Metabolic kinases moonlighting as protein kinases. Trends Biochem Sci 43: 301-310, 2018.
43. Iqbal MA, Gupta V, Gopinath P, Mazurek S and Bamezai RN: Pyruvate kinase M2 and cancer: An updated assessment. FEBS Lett 588: 2685-2692, 2014.
44. Li Z, Yang P and Li Z: The multifaceted regulation and functions of PKM2 in tumor progression. Biochim Biophys Acta 1846: 285-296, 2014.
45. Wong N, Ojo D, Yan J and Tang D: PKM2 contributes to cancer metabolism. Cancer Lett 356: 184-191, 2015.
46. Zheng M, Xing W, Liu Y, Li M and Zhou H: Tetramerization of SATB1 is essential for regulating of gene expression. Mol Cell Biochem 430: 171-178, 2017.
47. French AC, Luscher B and Litchfield DW: Development of a stabilized form of the regulatory CK2beta subunit that inhibits cell proliferation. J Biol Chem 282: 29667-29677, 2007.